Western Indian Ocean JOURNAL OF Marine Science

Volume 20 | Issue 1 | Jan – Jun 2021 | ISSN: 0856-860X

Western Indian Ocean JOURNAL OF Marine Science

Published biannually

Aims and scope: The *Western Indian Ocean Journal of Marine Science* provides an avenue for the wide dissemination of high quality research generated in the Western Indian Ocean (WIO) region, in particular on the sustainable use of coastal and marine resources. This is central to the goal of supporting and promoting sustainable coastal development in the region, as well as contributing to the global base of marine science. The journal publishes original research articles dealing with all aspects of marine science and coastal management. Topics include, but are not limited to: theoretical studies, oceanography, marine biology and ecology, fisheries, recovery and restoration processes, legal and institutional frameworks, and interactions/relationships between humans and the coastal and marine environment. In addition, *Western Indian Ocean Journal of Marine Science* features state-of-the-art review articles and short communications. The journal will, from time to time, consist of special issues on major events or important thematic issues. Submitted articles are subjected to standard peer-review prior to publication.

Manuscript submissions should be preferably made via the African Journals Online (AJOL) submission platform (http://www.ajol.info/index.php/wiojms/about/submissions). Any queries and further editorial correspondence should be sent by e-mail to the Chief Editor, wiojms@fc.ul.pt. Details concerning the preparation and submission of articles can be found in each issue and at http://www.wiomsa.org/wio-journal-of-marine-science/ and AJOL site.

ISSN 0856-860X

Cover image: The mudskipper *Periophthalmus argentilineatus* on the mangrove of Ulo Beach, Cabo Delgado, North Mozambique. © José Paula, 2006

Seasonal variability of vertical patterns in chlorophyll-*a* fluorescence in the coastal waters off Kimbiji, Tanzania

Nyamisi Peter[1,4] *, Masumbuko Semba[2], Charles Lugomela[2], Margareth Kyewalyanga[3]

[1] University of Dar es Salaam, PO Box 35061, Dar es Salaam, Tanzania

[2] Nelson Mandela African Institution of Science and Technology, PO Box 447, Arusha, Tanzania

[3] Institute of Marine Sciences, University of Dar es Salaam, PO Box 668, Zanzibar, Tanzania

[4] University of Dodoma, PO Box 338, Dodoma, Tanzania

* Corresponding author: nyamisip@gmail.com

Abstract

A study on the vertical pattern of chlorophyll-*a* (Chl-*a*) fluorescence was undertaken in the Mafia Channel off Kimbiji, Tanzania. Data was collected during the Southeast Monsoon (SEM) and Northeast Monsoon (NEM) seasons. There was higher Chl-*a* concentration of 0.1 to 1.1 mgm^{-3} in the surface layer off Kimbiji to about 50 m depth due to the presence of mixed layer depth (MLD) which allowed water mixing in the layer. A deep Chl-*a* maximum was recorded at around 40 m depth during the NEM and between 40 and 70 m in the SEM. Surface water between longitude 39.9°E and 40.2°E had low Chl-a from the surface to about 50 m depth due to poor nutrient input. The NEM had an insignificantly higher Chl-*a* value than the SEM (p > 0.05) which differed from other studies in which Chl-a was higher during the SEM than the NEM, than, the Chl-a concentration was higher at the surface during the SEM than during the NEM. Satellite data showed higher Chl-*a* in the SEM than NEM, localized along the Mafia Channel. During the SEM season the wind pushes higher Chl-*a* water from the Mafia Channel towards the north and leads to a higher concentration at Kimbiji.

Keywords: Chlorophyll-*a*, CTD, Kimbiji, Mafia Channel, monsoon season

Introduction

Phytoplankton are microscopic free–floating aquatic plants. They possess chlorophyll-*a,* a green pigment that absorbs light from the sun and converts it into energy through the photosynthetic process (Peter, 2013; Peter *et al*., 2018; Semba *et al*., 2016). The concentration of organic carbon associated with phytoplankton (usually expressed as mgm^{-3}) is commonly used to express the amount of phytoplankton (Cullen, 1982). Phytoplankton account for about half of global primary production (Boyce *et al*., 2010). They also serve as primary producers in marine environments and form the base of most aquatic food webs (Kyewalyanga *et al*., 2007; Semba *et al*., 2016). Phytoplankton provides food for herbivorous zooplankton and other invertebrates, fishes and large mammals, including whales (Roy, 2009). Further, phytoplankton regulates climate processes and bio-geochemical cycles through the carbon cycle (IPCC, 2014).

Chl-*a* found in phytoplankton is used as a proxy to determine the concentration of these microscopic plants in coastal and marine waters. Normally, surface waters have high Chl-*a* concentrations and thus contribute significantly to ocean productivity. However, high Chl-*a* concentration is not always found in the surface waters; sometimes they are subsurface, at greater depths, especially in areas with strong thermal stratification (Cullen, 1982). This type of Chl-*a* peak is referred to as the deep chlorophyll maximum (DCM) or subsurface Chl-*a* maximum. In the Western Indian Ocean, the DCM is reported to occur at around 50-75

http://dx.doi.org/10.4314/wiojms.v20i1.3

m depth (Conkright *et al.*, 1998; Owens *et al.*, 1993; Wiggert *et al.*, 2006).

The DCM is very important in ecology since it contains much of the world's primary production and facilitates nutrient cycling. This layer is an important food source for consumers as it has a higher concentration of primary producers at one location in the water column. In nutrient poor waters, the DCM accounts for more than half of the overall primary production due to phytoplankton growth (Macías *et al.*, 2014; Weston *et al.*, 2005). A high rate of primary production in the DCM facilitates nutrient cycling to higher trophic levels in the mixed layer. Studies shows that the DCM occurs at the same depth as the nutricline (Estrada *et al.*, 1993), thus phytoplankton at this layer can obtain nutrients coming up from deep waters. Phytoplankton in the DCM can then cycle back up the water column providing nutrients for other organisms in the mixed layer (Cullen, 2015). The DCM is therefore associated with predator-prey interactions, energy and biomass flow and biogeochemical cycles within the ecosystem (Leach *et al.*, 2018). Since most parts of Tanzanian coastal waters are nutrient poor and have oligotrophic characteristics, primary production might be concentrated in the subsurface waters, at the DCM. Thus, studies on vertical distribution of Chl-*a* and the dynamic of the DCM are important in understanding productivity potential in Tanzania coastal waters.

Until recently, most studies conducted in the coastal waters of Tanzania focused mainly on the abundance of phytoplankton in surface waters. For example (Lugomela *et al.*, 2002) examined biomass of colony forming *Trichodesmium* species and found higher biomass during the NE than the SE monsoon season. A study by Peter (2013) found higher Chl-*a* concentrations during the rainy season as compared to the dry season in the Zanzibar and Pemba Channels. Another study by Semba *et al.* (2016) assessed how the decrease in phytoplankton biomass in the Rufiji-Mafia Channel impacts on prawn catches. They found that the decline in Chl-*a* concentration was associated with the decrease in prawn catch in the Rufiji-Mafia Channel. Also, a study by Peter *et al.* (2018) showed how physical-chemical variables influence the spatial and seasonal variation of Chl-*a* in the coastal waters of Unguja, Zanzibar. They revealed that ammonia and nitrate were the major drivers of high Chl-*a* during the SE monsoon as compared to the NE monsoon season. Other studies used ocean colour satellite images and found that Chl-*a* levels are usually below 1 mgm^{-3} (Barlow *et al.*, 2011) and there is considerable variability with seasons in Tanzania waters (Semba *et al.*, 2016).

These previous studies widen our understanding of the dynamics of phytoplankton and Chl-*a* in the coastal and marine waters of Tanzania. However, these studies focused on phytoplankton at the surface of the ocean. Knowledge about vertical distribution and seasonal variability of Chl-*a* in coastal waters of Tanzania is lacking. Also, there is paucity of knowledge on forces that control phytoplankton abundances. Preliminary investigations of the vertical structure of Chl-*a* and environmental variables (temperature, salinity) were undertaken during the Tanzanian leg of the Second International Indian Ocean Expedition (IIOE-2) in early November 2017 and June 2018. This study intended to investigate: (1) vertical variation in Chl-*a* concentration off Kimbiji during the two monsoon seasons; (2) seasonal variation in the mixed layer depth; and (3) environmental factors influencing seasonal variation in Chl-*a* concentration off Kimbiji.

Materials and methods

Study area

This study was conducted in the coastal water off Kimbiji, located between longitude 39.3°E and 40.3°E and latitude 8°S and 6.8°S (Fig. 1). The area is about 40 km southeast of Dar es Salaam's city center and bordered by the Mafia Channel in the south. The area was selected because there were no phytoplankton records for this site. The other reason for picking this area was because the area contains two transect with hydrographic profile data of temperature, oxygen, salinity, chlorophyll fluorescence and turbidity recorded during the 2017 and 2018 International Indian Ocean Expedition 2 (IIOE-2). The first transect has four sampling stations recorded during the SE monsoon season of 2018, while the second transect has eight sampling stations with similar profiles as the first transect recorded during the NE monsoon season of 2017 (Fig. 1).

The monsoon season influences the climate of the study area. The NE monsoon season runs from November to March and the SE spans from May to September (Semba *et al.*, 2019). The monsoon seasons have a marked effect on air and water temperature, winds and rainfall (Mahongo *et al.*, 2011; Richmond, 2011). Winds are a particularly important feature of the Western Indian Ocean, driving water circulation and affecting wave action, local climate, biological processes and human activities (Richmond, 2011). The trade winds are steady and light, blowing from the northeast towards the southwest at about 5 ms^{-1} during NE monsoon season. The NE monsoon is associated with the short rainy period (October–December). The long rainy season begins after the NE monsoon season from March to June. Trade winds reverse during the SE monsoon and blow from the southeast towards the northwest at a relatively strong speed of about 9 ms^{-1}, associated with cooler temperature and rough ocean. During April and October the ocean is calm, with moderate temperatures forming during the inter-monsoon seasons. The seasonal reversal of monsoon winds influences phytoplankton distribution in this region (George *et al.*, 2013; Mahongo *et al.*, 2011; Richmond, 2011). The reverse of the monsoon winds regulates mixing in the ocean that affects nutrient flux across the thermocline and the distribution of Chl-*a* concentration. Air temperature in the study area rarely fall below 20 °C and the seawater temperature reaches a minimum of 25 °C in September and maximum of 29 °C in March (McClanahan, 1988; Peter, 2013).

Data collection

Conductivity–temperature–depth (CTD)

Data for this study was collected during the 2017 and 2018 International Indian Ocean Expedition 2 (IIOE-2) onboard Agulhas II, respectively for the NE and SE monsoon seasons. Data for the NE and SE monsoon seasons were collected in November 2017 and June 2018, respectively, with all samples taken from the coastal waters of Tanzania. The vertical profile of temperature and fluorescence were recorded with a CTD (Seabird 11 plus, Seabird Electronics, USA). The spatial information of the sampling locations is shown in Figure 1 and Table 1.

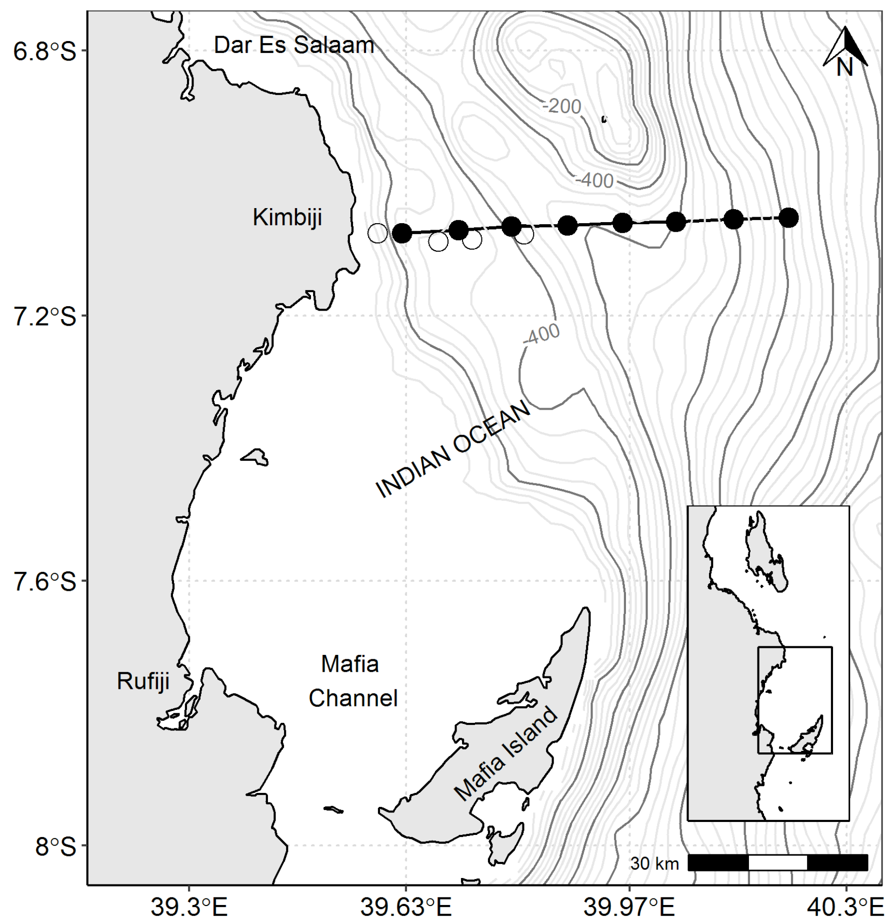

Figure 1. Map showing the location of the transect off Kimbiji located on the northern side of the Mafia Channel. The grey solid lines are contours at 50 m interval and solid black lines are contours at 200 m. The black filled points show the stations for the NE monsoon and the black hollowed points show stations for the SE monsoon season. The inset map shows the location of the study area in the coastal waters of Tanzania.

Table 1. Table showing location of the CTD cast off the Kimbiji transect.

Date	Time	Longitude	Latitude
2017-11-05	23:29:37	40.2117	-7.0525
2017-11-06	03:57:19	40.1283	-7.0543
2017-11-06	05:26:03	40.0407	-7.0587
2017-11-06	08:00:43	39.9592	-7.0600
2017-11-06	09:25:07	39.8750	-7.0642
2017-11-06	14:52:20	39.7897	-7.0658
2017-11-06	16:07:12	39.7095	-7.0710
2017-11-06	18:47:34	39.6238	-7.0755

Surface drifters

Drifter data was used to assess the influence of ocean currents on the seasonal and spatial distribution of Chl-*a* fluorescence. Drifter data was obtained from the Global Drifter Program as a text file and was used to compute surface current speed and direction in the study area. The ocean currents were then grouped and averaged between the NE and SE monsoon.

Satellite data

To complement distribution of Chl-*a* both in space and season, satellite derived chlorophyll data was used. The level 3 monthly Chl-*a* concentrations were downloaded from MODIS with a spatial resolution of 4 km from September 2017 to August 2018. To understand the association between Chl-*a* and sea surface temperature (SST), sea surface temperature with the same resolution and time period was downloaded from MODIS. Surface wind data was also downloaded from QuikSCAT.

Data processing

The raw CTD data was converted to the *.cnv* file format using the Sea Bird (SBE) software and then processed in R-language using the **oce** package (Kelly and Richards, 2018). Because of the large number of profiles, the processing of CTD data was iterated. The process involved several steps. First, a list of all CTD files in the working directory was created in the R-working directory using the *dir()* function. Second, a dummy file that stored CTD files was then constructed using the *list()* function. After that, each file in the working directory was imported with the *read.ctd()* function. Only the downcast values of the CTD profiles were used for analysis.

To determine the mixed layer depth (MLD), the method described by (Chu and Fan, 2010) was applied. Here, successively deeper data points in each of the profile potential temperatures is examined until one is found with a potential temperature value differing from the value at the 10 m reference depth by more than the threshold value (δT) of $\pm$ 0.5 °C. 0.5 °C. To understand the influence of vertical structure, fluorescence profiles were divided into stratum of 50 meter intervals from the surface to 200 meter depth. The difference in mean Chl-*a* concentration between seasons and among strata was computed with general linear modelling and the multiple comparison between the seasons was calculated with Tukey's HSD test.

The monthly satellite sea surface temperature (SST) and Chl-*a* as well as wind speed and direction were converted into tabular data and averaged for the NE and SE monsoon seasons. The average SST and Chl-*a* were used to map distribution patterns of temperature and Chl-*a* both in space and season in the study area. The surface current, wind speed and direction were overlaid into seasonal maps of temperature and Chl-*a* to examine their influence on the distribution of temperature and Chl-*a* within the study area. Drifters were also aligned to the NE and SE monsoon season and mapped against the Kimbiji transect to examine the pathway of surface water across a transect. The data processing, analysis, plotting and mapping was done in the R environment.

Results

Vertical profiles of temperature and Chl-*a*

The vertical profiles of Chl-*a* and temperature during the NE and SE monsoon seasons off the Kimbiji

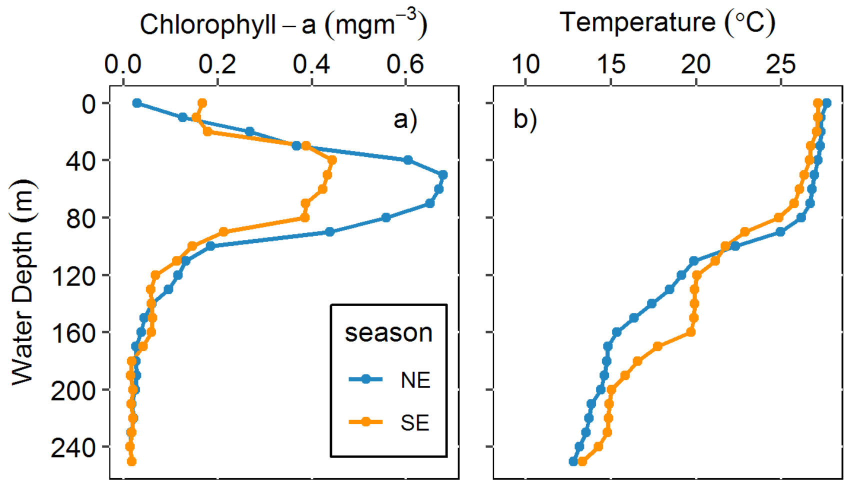

Figure 2. Vertical profiles of *in-situ* a) chlorophyll-*a*, and b) temperature off the Kimbiji coast measured in November 2017 (NE) and June 2018 (SE).

coast near longitude 39.7095°E and latitude7.0755°S are shown in Figure 2a and 2b. Chl-*a* profiles showed a marked difference during the two monsoon seasons (Fig. 2a). Figure 2 indicates that while the surface water has almost uniform temperature, Chl-*a* values differ with season. Chl-*a* profiles at Kimbiji show lower values at the surface with concentration values of less than 0.1 mgm^{-3} during the NE monsoon season and about 0.17 mgm^{-3} in the SE monsoon season (Fig. 2a). These values were uniform to about 20 m depth, where they started to increase sharply and reached a maximum concentration of 0.44 mgm^{-3} at 40 m depth during the SE monsoon season. There was a slow decline in concentration from 40 m to 80 m depth where Chl-*a* started to decline sharply reaching nearly 0 mgm^{-3} at the bottom in the SE monsoon season. During the NE monsoon, Chl-*a* concentration increased sharply from about 0.02 mgm^{-3} at the surface to a maximum concentration of about 0.7 mgm^{-3} at 50 m depth at Kimbiji (Fig. 2a). Chl-*a* then decreased sharply from 0.7 mgm^{-3} at 50 m to about 0.19 mgm^{-3} at 100 m depth and remained relatively low and constant with increasing depth, reaching nearly 0 mgm^{-3} at the bottom in the NE monsoon. Chl-*a* was slightly higher in the upper 30 m during the SE monsoon (mean ± SE = 0.222 ± 0.0555) than during the NE monsoon (0.198 ± 0.075) (t = -0.26, df = 5.53, p = 0.80; Fig. 2a). However, in the 30-80 m water layer, Chl-*a* values were significantly higher during the NE monsoon season (0.59 ± 0.05) than during the SE monsoon

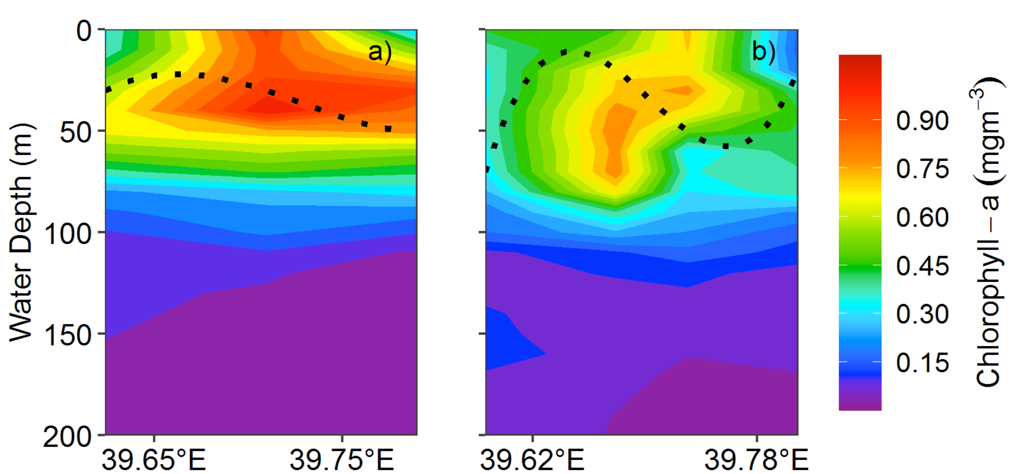

Figure 3. Longitudinal cross-section of chlorophyll-a within a 200 meter water column off Kimbiji during a) the NE and b) SE monsoon season. The black dotted lines show the location of the MLD for each season.

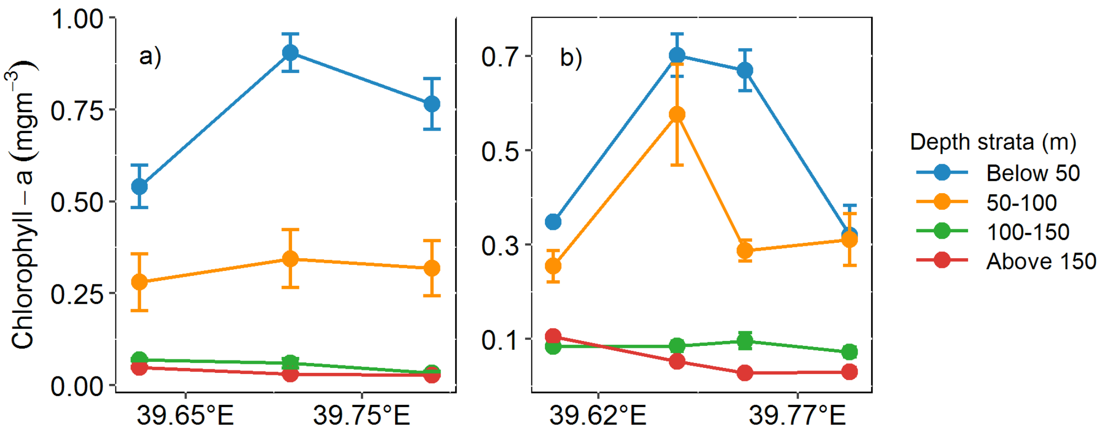

Figure 4. Chlorophyll-a distribution along the Kimbiji transect stratified into depth groups during a) the NE and b) SE monsoon seasons.

(0.41 ±0.01) (t = 3.63, df = 5.51, p = 0.01). The temperature profiles indicate that water temperatures were slightly higher during the NE monsoon season with nearly uniform water temperatures from the surface to about 80 m depth (Fig. 2b). Water temperature decreased gradually from ~28 °C near the surface to about 25 °C at about 80 m depth and then decreased sharply to about 14 °C at 120 m, followed by a gradual decrease to the lowest temperature at 240 m.

Seasonal cross-sections of Chl-*a*

To address the effect of physical processes on Chl-*a* distribution off Kimbiji, the vertical distribution of Chl-*a* in the upper 200 m of the water column and the mixed layer depth were analyzed during the SE and NE monsoon season. Figure 3a and b show that the vertical structure of Chl-*a* concentration varies with monsoon season and depth. During the NE monsoon, the water from the surface to about 75 m depth has relatively higher Chl-*a* concentrations ranging between 0.1 and 1.1 mgm^{-3} (Fig. 3a). The values for Chl-*a* concentration then increased with depth from the coastline toward offshore (Fig. 3a). The bottom water above 90 m was relatively low in Chl-*a* concentration and ranged between 0.01 to 0.2 mgm^{-1} (Fig. 3a). Similarly, during the SE monsoon season, water had a Chl-*a* concentration ranging between 0.5–0.8 mgm^{-3} along the transect from the surface to about 75 m depth (Fig. 3b), with peak values near longitude 39.68°E. The concentration of Chl-*a* was below 0.3 mgm^{-3} for water above 90 m depth (Fig. 3b). The mixed layer depth (MLD) pattern varies between the NE (Fig. 3a) and SE (Fig. 3b) monsoon seasons. The MLD during the NE monsoon ranged between 22.2 and 49.8 m depth with the MLD of about 42 m with a maximum Chl-*a* concentration (~1.03 mgm^{-3}) (Fig. 3a). During the SE monsoon, the MLD ranged between 20 to 70 m and there was an unclear pattern between MLD and Chl-*a* concentration (Fig. 3b).

Seasonal and depth variation of Chl-*a*

Figure 4a and b show the Chl-*a* concentration along the transect divided into four depth groups during the two monsoon seasons. During the NE monsoon season, the stratum below 50 m depth had relatively higher Chl-*a* concentration (0.5–0.9 mgm^{-3}) followed by the 50-100 m strata (0.28 and 0.35 mgm^{-3}). The remaining two water layers (100-150 and 150-200 m depth) had low concentrations below 0.2 mgm^{-3} (Fig. 4a). Similarly, the SE monsoon had higher Chl-*a* concentrations in water below 50 m depth, which ranged between 0.35 and 0.7 mgm^{-3} compared to the other depth strata (Fig. 4b). The 50-100 m stratum had slightly lower concentrations than the surface stratum. The 100–150 and 150–200 m strata had concentrations below 0.1 mgm^{-3}.

Figure 5a and b show seasonal variation of Chl-*a* concentrations within the upper 50 m (Fig. 5a) and 50–100 m water layers (Fig. 5b). Both strata had insignificantly higher Chl-*a* concentration during the NE as compared to the SE monsoon season (t = -1.053, p = 0.3). However, the concentration of Chl-*a* at station 2 of the 50–100 m water layer was relatively higher during the SE monsoon (~0.58 mgm^{-3}) than during the NE monsoon season (~0.34 mgm^{-3}).

Seasonal temperature cross section

Figure 6a and b show the vertical structure of temperature off the Kimbiji transect in relation to monsoon seasons. In both the NE and SE monsoon season, the

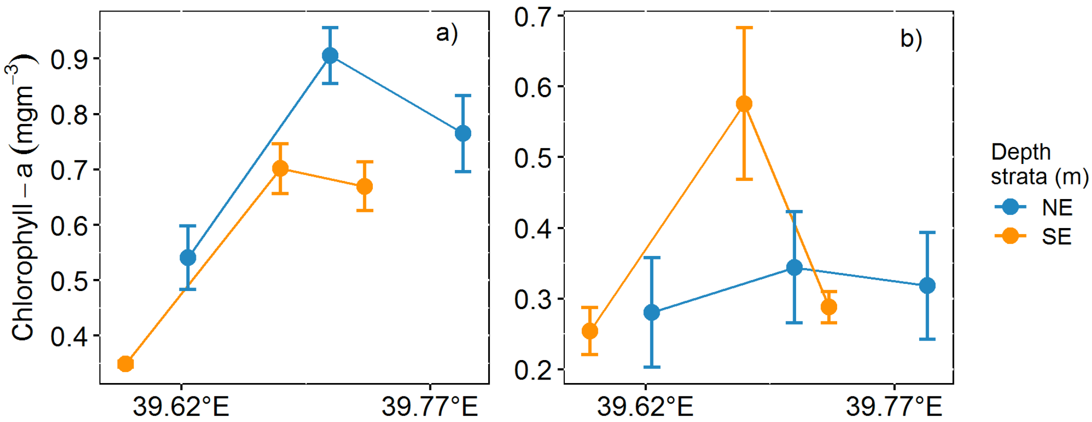

Figure 5. Mean and standard error of chlorophyll-a concentration at Kimbiji divided into strata of a) surface to 50 meter depth, b) 50-100 meter for the NE and SE monsoon seasons.

surface water layer below 75 m depth was very warm (26–28 °C) compared to bottom waters (Fig. 6). However, surface water temperature during the NE monsoon (Fig. 6a), was slightly higher (~28 °C) than that of the SE (~27°C) monsoon season (Fig. 6b). The thermocline during the NE monsoon was shallower at around 80 m depth indicated by a sharp decrease in temperature from 24 to 18 °C. Below the thermocline, temperature decreased gradually from 18 °C to 14 °C at 200 m. For the SE monsoon season, the thermocline was present at about 100 m depth (Fig. 6b), below which temperature decreased to the lowest (16 °C) at 200 m.

Seasonal and spatial variation of surface Chl-*a* and SST

The MODIS satellite data was used to map seasonal distribution patterns of surface SST and Chl-*a* within the study area. Figure 7 shows that the SE monsoon had a relatively higher Chl-*a* concentration (Fig. 7b) than the NE monsoon season (Fig. 7a). The nearshore waters within the Mafia Channel had higher Chl-*a* concentrations than those further from the coastline (Fig. 7a and b). The wind vector arrows show a north-westerly direction during the SE monsoon which pulls the channel water northwards spreading high Chl-*a* water in the channel and even further north off Kimbiji (Fig. 7b). The reversal of wind direction to south-westerly during the NE monsoon prevents the productive waters in the Mafia channel from moving further north, thus making the water off Kimbiji less productive at this time (Fig. 7a).

Figure 8a and b show the sea surface temperature patterns over season and space, indicating that the NE season has warmer temperatures (Fig. 8a) than the SE monsoon season (Fig. 8b). During the NE, SST ranged between 28 and 31° C, which was relatively higher compared to the 26 to 28° C observed during the SE

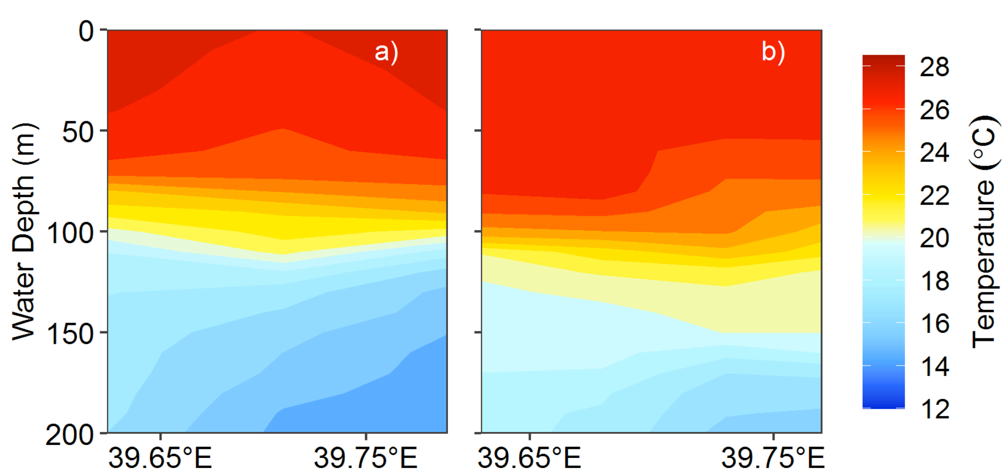

Figure 6. The hydrographic section of temperature at Kimbiji during a) NE and b) SE monsoon seasons.

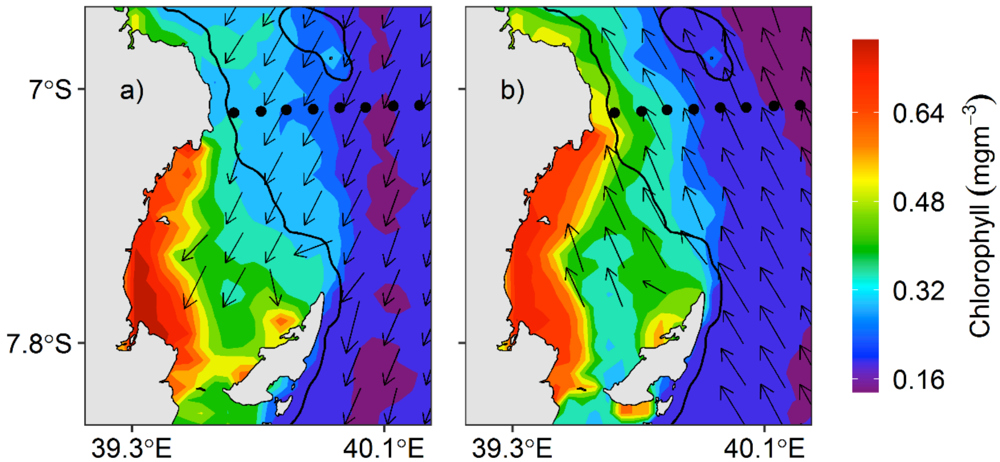

Figure 7. The seasonal surface chlorophyll-a overlaid on wind vectors of trade winds during a) the NE and b) SE monsoon seasons. The black solid line represents the isobaths at 200 m.

monsoon season. Furthermore, patches of very high temperature of about 31°C was observed off thet Rufiji River delta during the NE monsoon season (Fig. 8a).

Figure 9a and b show the seasonal averaged surface currents of the East Africa Coastal Current (EACC). The surface current shows northward propagation during the NE (Fig. 9a) and SE monsoon seasons (Fig. 9b). The pathways of the EACC align well with water of low Chl-*a* concentration and mark a clear distinction between the high and low Chl-*a* waters during the NE and SE monsoon season (Fig. 9a and b), respectively.

The vertical section in Figure 10 shows a cross–section of Chl-*a* along the transect presented in Figure 9. It shows that surface water within the path of the EACC (between longitude 39.8°E and 40.2°E) has relatively low Chl-*a* values compared to the coastal waters (longitude below 39.8°E).

Discussion

This study provides information on the vertical distribution of Chl-*a* in coastal marine waters of Tanzania. The study reports for the first time on the presence of a seasonal subsurface peak of Chl-*a* concentration in these waters. High surface Chl-*a* values were measured during the SE monsoon season unlike during the NE season, where the Chl-*a* concentration was slightly low (Fig. 2). Also, for the first time, this study relates Chl-*a* concentrations to the effect of the EACC where it was found that Chl-*a* was appreciably lower within the limits of this important current, regardless of

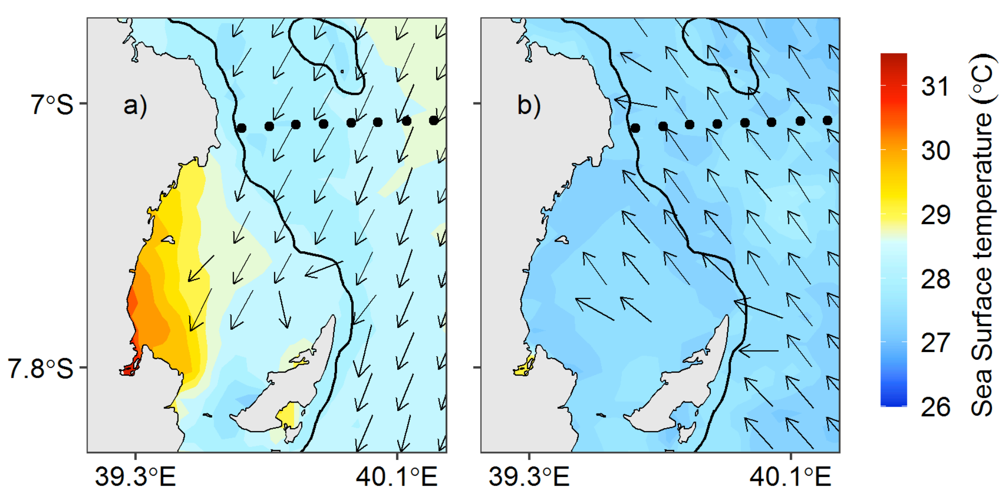

Figure 8. The seasonal surface temperature overlaid on wind vectors of trade winds during a) the NE and b) SE monsoon seasons. The black solid line represents the isobaths at 200 m.

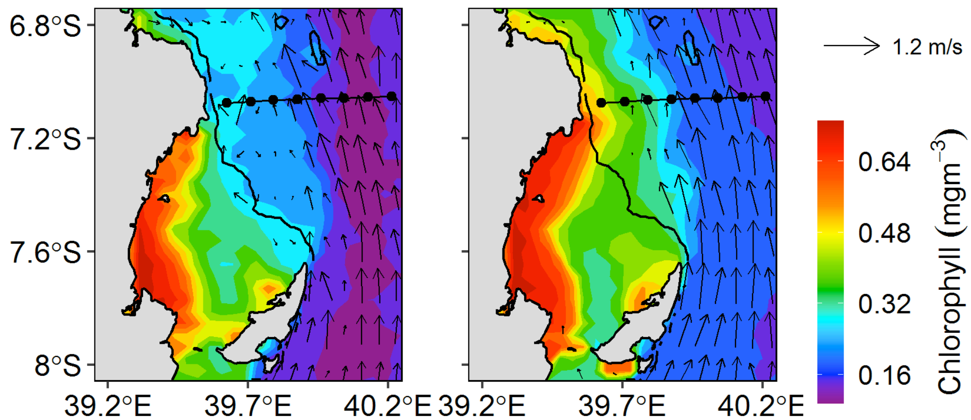

Figure 9. Vector arrows showing the speed and direction of East African Coastal Current (EACC) superimposed on surface chlorophyll-a during a) the NE and b) SE monsoon season. The black solid line represents the isobaths at 50 m.

season. In contrast, however, the nearshore areas had relatively higher Chl-*a* concentrations, attesting to the oligotrophic nature of the EACC, which is known to transport nutrient-poor water throughout the year (Mahongo and Shaghude, 2014).

The subsurface waters below 75 m depth off Kimbiji had relatively higher Chl-*a* values, which ranged between 0.1 and 1.1 mgm^{-3} during the NE and SE monsoon seasons (see Fig. 3). However, Chl-*a* values were relatively lower during the SE monsoon than during the NE monsoon season. Vertical distribution of Chl-*a* is governed by the thermal structure of the water column (Fig. 2) and other factors facilitating vertical mixing (Valenti *et al.*, 2015) such as vertical diffusivity which allows nutrients across the thermocline, light penetration or availability, nutrients availability in the productive layer (Cullen, 1982), and the variability of the mixed layer (see Fig. 3; Cullen ,1982; Valenti *et al.*, 2015). Nevertheless, the Chl-*a* maximum (DCM) was found close to 40 m depth and between 40 and 80 m during the NE and SE monsoon seasons, respectively. This is similar to the DCM depth reported in subtropical waters of the Western Indian Ocean (Conkright *et al.*, 1998; Owens *et al.*, 1993; Wiggert *et al.*, 2006). However, shallower DCM depths ranging between 25 and 47 m have been reported in the Bering Sea, and that currents, rather than nutrients, were the main driver of Chl-*a* spatial distribution (Cullen, 1982).

While nutrient concentration and light intensity may govern the vertical distribution of Chl-*a* in the marine environment, internal wave oscillations and Langmuir circulations have been shown to determine the dynamics of Chl-*a* within the thermocline and in the upper 5 m of the water column, respectively (George *et al.*, 2013). Also, Valenti *et al.* (2015) observed that while light is plentiful in surface waters, nutrients become a limiting factor for phytoplankton growth because of poor mixing. Similarly, at depths, light

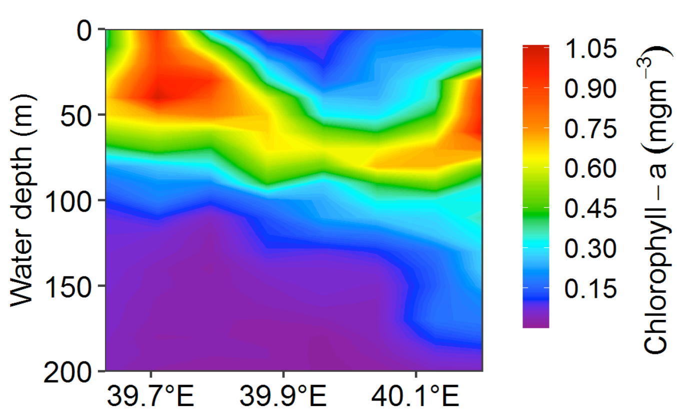

Figure 10. Hydrographic section showing chlorophyll-a concentration in the water column along the transect off Kimbiji.

becomes limiting while nutrient concentrations are high maintaining an increase in Chl-*a* within the photic layer (Cullen, 1982; Valenti *et al.*, 2015).

Chl-*a* concentration showed significant seasonal variation in different water layers (Fig. 4). The surface water layer (below 50 m) had the highest Chl-*a* concentration, followed by the water layer within 50–100 m (Fig. 4a and b), while water above 100 m depth had the lowest Chl-*a* values (Fig. 4). The reason for higher Chl-*a* concentration at these two surface strata is because the MLD is located within these strata; that is at 22.2 to 49.8 m and 20 to 70 m depth during NE (Fig. 3a) and in SE monsoon season (Fig. 3b), respectively. The MLD is important as it helps nutrient enrichment to the surface thereby increasing Chl-*a* concentration and also allows phytoplankton distribution in the mixed layer (George *et al.*, 2013; Vinayachandran and Saji, 2008; Waliser *et al.*, 2005)

It was surprising that the NE had an insignificantly higher Chl-*a* value than the SE monsoon season for water below 50 m and between 50 and 100 m (Fig. 5a and b; $p > 0.05$). This finding is opposite to previous studies, which found a higher Chl-*a* value during the SE as compared to the NE monsoon season (Limbu and Kyewalyanga, 2015; Peter *et al.*, 2018; Semba *et al.*, 2016). While these previous studies focused on Chl-*a* variation at the surface of the ocean (less than 5 m depth), the present study dealt with Chl-*a* throughout the water column which had higher subsurface Chl-*a* concentration in the NE than SE monsoon season. This might account for the difference observed (Fig. 2).

Contrary to the hydrographic section of Chl-*a*, the surface Chl-*a* value from the satellite clearly showed the SE season had relatively higher Chl-*a* value than the NE monsoon season (Fig. 7). The Chl-*a* pattern over the study area indicates a relatively higher value in the Mafia Channel, which is confined within shallow waters below 200 m depth (Fig. 7). The relatively colder waters and northwesterly wind (Fig. 8b) during the SE monsoon season provides sufficient surface mixing which is conducive for elevated productivity in this area. This productive water is pushed northwards by the trade winds during SE monsoon season and transports high Chl-*a* concentration waters towards the Kimbiji segment (Fig. 7b). However, the reversing wind during the NE monsoon season prevents transport of high Chl-*a* value water toward the Kimbiji segment, leading to a low value of surface Chl-*a* at this time of the year (Fig. 7a). The Mafia Channel is unaffected by the EACC, which passes in waters deeper than 200 m, just offshore of Mafia Island. A previous study in the Mafia Channel indicated similar findings and found nutrient input from the Rufiji River to be important in this area (Semba *et al.*, 2016).

Although the surface water is well lit, the water between longitude 39.9°E and 40.2°E has relatively low Chl-*a* value from the surface to nearly 50 m depth (Fig. 10). This indicates that less–productive surface water along this section is mainly caused by the flushing of nutrient–poor, high salinity, and relatively warm water (Figure A1), which is dragged across the area by the EACC (Fig. 9). However, high Chl-*a* values recorded at stations close to the coast are supported by both the hydrographic section (Fig. 10) and surface Chl-*a* from satellite data (Fig. 7).

Information on the vertical distribution pattern of Chl-*a* in Tanzanian coastal and marine waters is limited, partly due to the absence of reliable data from within the water column. Missions such as the RV Algoa cruise and the second International Indian Ocean Expedition conducted in the Western Indian Ocean provided the CTD profile data used in this study. The results show that the EACC affects Chl-*a* values in the area between longitude 39.9°E and 40.2°E. These low Chl-*a* values are caused by flushing of nutrient-poor, high salinity, and high temperature water pulled across this area by the EACC. The study also found that the NE had higher Chl-*a* value than the SE monsoon season which was different from other studies in Tanzania. But when considering only the surface of the ocean, as was done in previous studies, then the SE had higher concentrations than NE. Also, the satellite surface Chl-*a* showed higher concentrations in the SE as compared to the NE monsoon season. Although the CTD data from different missions have helped research into the study of physical, chemical and biological variability of the water column in the ocean, continuous data collection is missing. This information could help in understanding short and long-term changes of the ocean throughout the water column.

The upper ocean is characterized by a quasi-homogeneous layer where temperature, salinity and density are almost constant with increasing depth (Costoya *et al.*, 2014). This homogeneity is caused by turbulent vertical mixing that is driven by heat loss from the ocean to the atmosphere, as well as by wind stress (Stranne *et al.*, 2018). The deepest layer affected by this turbulent mixing is called the mixed layer depth

(MLD), which marks the section of the upper ocean that interacts with the atmosphere (Kelly and Richards, 2018). The MLD influences the exchange of heat and gases between the atmosphere and the ocean and constitutes one of the major factors controlling ocean primary production as it affects the vertical distribution of biological and chemical components in near-surface waters. Estimation of the MLD are often made by means of conductivity, temperature and depth (CTD) casts (Stranne *et al*., 2018). However, different techniques are used and there is little agreement on which technique is the best for estimating MLD (Kelly and Richards, 2018).

Acknowledgements

We are grateful to the second International Indian Ocean Expedition and the RV Algoa cruise for giving us permission to use their data. We are thankful to the MODIS for providing the satellite SST and chlorophyll-*a* data used in this study. We are also grateful to the Global Drifter Program for allowing us access to the drifter data that was used to calculate the ocean surface currents. The QuikSCAT is highly acknowledged for the permission to access the surface wind data.

References

Barlow R, Lamont T, Kyewalyanga M, Sessions H, Berg M, van Den FD (2011) Phytoplankton production and adaption in the vicinity of Pemba and Zanzibar Island, Tanzania. African Journal of Marine Sciences 33: 283-295

Boyce DG, Lewis MR, Worm B (2010) Global phytoplankton decline over the past century. Nature 466: 591-6 [https://doi.org/10.1038/nature09268]

Chu P, Fan C (2010) Optimal linear fitting for objective determination of ocean mixed layer depth from glider profiles. Journal of Atmospheric and Ocean Technology 27: 1893-1898

Conkright M, O'Brien T, Levitus S, Boyer T, Stephens C, Antonov J (1998) World ocean atlas 1998. Vol. 12 of NOAA Atlas, Nesdis

Costoya X, deCastro M, Gomez-Gesteira M, Santos F (2014) Mixed layer depth trends in the Bay of Biscay over the period 1975-2010. PloS One 9: e99321

Cullen JJ (1982) The deep chlorophyll maximum: Comparing vertical profiles of chlorophyll a. Canadian Journal of Fisheries and Aquatic Sciences 39: 791-803

Cullen JJ (2015) Subsurface chlorophyll maximum layers: Enduring enigma or mystery solved? Annual reviews

Estrada M, Marrasé C, Latasa M, Berdalet E, Delgado M, Riera T (1993) Variability of deep chlorophyll maximum characteristics in the Northwestern Mediterranean. Marine Ecology Progress Series: 289–300

George JV, Nuncio M, Chacko R, Anilkumar N, Noronha SB, Patil SM, Pavithran S, Alappattu DP, Krishnan K, Achuthankutty C (2013) Role of physical processes in chlorophyll distribution in the western tropical Indian Ocean. Journal of Marine Systems 113: 1-12

IPCC (2014) Impacts, adaptation, and vulnerability. Part a: Global and sectoral aspects. Contribution of working group II to the fifth assessment report of the intergovernmental panel on climate change. 1132 pp

Kelly D, Richards C (2018) Oce: Analysis of oceanographic data.

Kyewalyanga M, Naik R, Hegde S, Raman M, Barlow R, Roberts M (2007) Phytoplankton biomass and primary production in Delagoa Bight Mozambique: Application of remote sensing. Estuarine, Coastal and Shelf Science 74, 429-436 [https://doi.org/10.1016/j.ecss.2007.04.027]

Leach TH, Beisner BE, Carey CC, Pernica P, Rose KC, Huot Y, Brentrup, JA, Domaizon I, Grossart HP, Ibelings BW (2018) Patterns and drivers of deep chlorophyll maxima structure in 100 lakes: The relative importance of light and thermal stratification. Limnology and Oceanography 63: 628-646

Limbu SM, Kyewalyanga MS (2015) Spatial and temporal variations in environmental variables in relation to phytoplankton composition and biomass in coral reef areas around Unguja Island, Tanzania. Journal of SpringerPlus 4: 1-18

Lugomela C, Lyimo T, Bryceson I, Semesi A, Bergman B (2002) *Trichodismium* in coastal waters of Tanzania: Diversity, seasonality, nitrogen and carbon fixation. Hydrobiologia 477: 1-13

Macías D, Stips A, Garcia-Gorriz E (2014) The relevance of deep chlorophyll maximum in the open Mediterranean Sea evaluated through 3D hydrodynamic-biogeochemical coupled simulations. Ecological Modelling 281: 26-37

Mahongo SB, Francis J, Osima SE (2011) Wind patterns of coastal Tanzania: Their variability and trends. Western Indian Ocean Journal of Marine Science 10: 107-120

Mahongo S, Shaghude Y (2014) Modelling the dynamics of the Tanzanian coastal waters. Journal of Oceanography and Marine Science 5: 1-7 [https://doi.org/10.5897/JOMS2013. 0100]

McClanahan T (1988) Seasonality in east Africa's coastal waters. Marine Ecology Progress Series 44: 191-199

Owens N, Burkill P, Mantoura R, Woodward E, Bellan I, Aiken J, Howland R, Llewellyn C (1993) Size-fractionated primary production and nitrogen assimilation in the northwestern Indian Ocean. Deep Sea Research Part II: Topical Studies in Oceanography 40: 697-709

Peter N (2013) Phytoplankton distribution and abundance along the Zanzibar and Pemba Channels. MSc Thesis, University of Dar es Salaam 104 pp

Peter N, Semba M, Lugomela C, Kyewalyanga M (2018) The influence of physical-chemical variables on the spatial and seasonal variation of chlorophyll-a in coastal waters of Unguja, Zanzibar, Tanzania. Western Indian Ocean Journal of Marine Science 17: 25-34

Richmond MD (2011) A field guide to the seashores of Eastern Africa and the Western Indian Ocean Islands. Sida/WIOMSA. 464 pp

Roy S (2009) Do phytoplankton communities evolve through a self-regulatory abundance–diversity relationship? BioSystems 95: 160-165

Semba M, Kimirei I, Kyewalyanga M, Peter N, Brendonck L, Somers B (2016) The decline in phytoplankton biomass and prawn catches in the Rufiji-Mafia Channel, Tanzania. Western Indian Ocean Journal of Marine Science 15: 15-29

Semba M, Lumpkin R, Kimirei I, Shaghude Y, Nyandwi N (2019) Seasonal and spatial variation of surface current in the Pemba Channel, Tanzania. PLoS One 14: e0210303 [https://doi.org/10.1371/journal.pone.0210303]

Stranne C, Mayer L, Jakobsson M, Weidner E, Jerram K, Weber TC, Anderson LG, Nilsson J, Björk G, Gårdfeldt K (2018) Acoustic mapping of mixed layer depth. Ocean Science 14: 503-514

Valenti D, Denaro G, Spagnolo B, Conversano F, Brunet C (2015) How diffusivity, thermocline and incident light intensity modulate the dynamics of deep chlorophyll maximum in Tyrrhenian Sea. PLoS One 10: 1–31 [https://doi.org/10.1371/journal.pone.0115468]

Vinayachandran P, Saji N (2008) Mechanisms of South Indian Ocean intraseasonal cooling. Geophysical Research Letters 35 (23): L23607

Waliser DE, Murtugudde R, Strutton P, Li JL (2005) Subseasonal organization of ocean chlorophyll: Prospects for prediction based on the madden-Julian oscillation. Geophysical Research Letters 32 (23): L23602

Weston K, Fernand L, Mills D, Delahunty R, Brown J (2005) Primary production in the deep chlorophyll maximum of the central North Sea. Journal of Plankton Research 27: 909-922

Wiggert J, Murtugudde R, Christian J (2006) Annual ecosystem variability in the tropical Indian Ocean: Results of a coupled bio-physical ocean general circulation model. Deep Sea Research Part II: Topical Studies in Oceanography 53: 644-676

Appendix

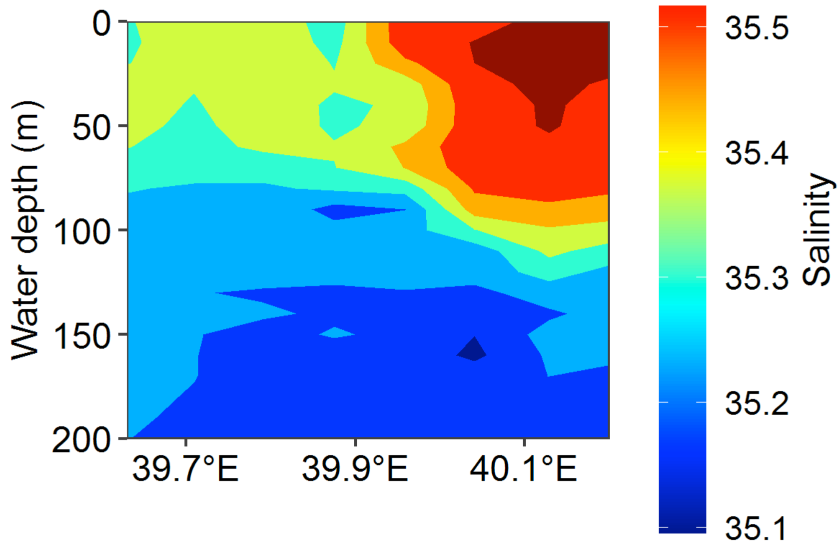

Figure A1. Hydrographic section showing the salinity in the water column along the transect off Kimbiji.